第 30 卷第 8 期 无 机 化 学 学 报 Vol.30 No.8
2014 年 8 月 CHINESE JOURNAL OF INORGANIC CHEMISTRY 1969-1976

不同形貌纳米 $CoWO_4$ 的水热法制备及气敏性能

蒋东丽*,[1] 刘汉甫[1] 刘 峰[2] 白先群[1] 顾生玖[1]
([1]桂林医学院药学院,桂林 541004)
([2]安徽工业大学化学与化工学院,马鞍山 243002)

摘要: 以 $Co(NO_3)_2·6H_2O$、$Na_2WO_4·2H_2O$ 为主要原料,去离子水为溶剂,利用水热法在不同条件下制备了一系列的纳米 $CoWO_4$,用 XRD、TEM 和比表面分析仪对产品的物相、形貌和比表面积进行了表征。较系统地探讨了水热条件(反应混合物 pH 值、反应时间、反应温度等)对产物物相和形貌的影响,并研究了不同形貌产品对甲醛、乙醇、氨气、苯和丙酮等的敏感性能。结果表明:水热条件对产品的物相和形貌有影响,在不同水热条件下,可成功制备 $CoWO_4$ 纳米颗粒、纳米立方体及纳米棒;以纳米颗粒、纳米立方体及纳米棒样品制成的气敏元件对被试气体有不同程度的响应, 其中以纳米颗粒为基的元件在 210 ℃对 1 000 μL·L^{-1} NH_3 灵敏度为 3.3。

关键词: $CoWO_4$; 水热法; 纳米棒; 纳米立方体; 气敏性能
中图分类号: TB34 **文献标识码**: A **文章编号**: 1001-4861(2014)08-1969-08
DOI: 10.11862/CJIC.2014.251

Hydrothermal Synthesis and Gas-Sensing Property of Nano-$CoWO_4$ with Different Morphologies

JIANG Dong-Li*,[1] LIU Han-Fu[1] LIU Feng[2] BAI Xian-Qun[1] GU Sheng-Jiu[1]
([1]*Pharmacy College, Guilin Medical University, Guilin, Guangxi* 541004, *China*)
([2]*School of Chemistry and Chemical Engineering, Anhui University of Technology, Maanshan, Anhui* 243002, *China*)

Abstract: $CoWO_4$ nanoparticles, nanocubes and nanorods were prepared by a facile hydrothermal process with $Co(NO_3)_2·6H_2O$, $Na_2WO_4·2H_2O$ as the main raw materials and distilled water as the solvent.The phase composition, the morphology and the specific surface area of the products were characterized by XRD, TEM and N_2 absorption-desorption. The influence of pH value, reaction temperature and reaction time on the morphology of the products was discussed in detail. The gas-sensing responses of $CoWO_4$ nanomaterials to HCHO, C_2H_5OH, NH_3, C_6H_6 and CH_3COCH_3 were investigated. The results demonstrate that pH value, reaction temperature and reaction time of hydrothermal process play a key role in the formation of different morphologies. The gas sensors based on the as-prepared $CoWO_4$ nanoparticles, nanocubes and nanorods samples exhibit responses to all the tested gases from 120 ℃ to 300 ℃. A noteworthy result is that the sensitivity of sensor based on the $CoWO_4$ nanoparticles is 3.3 at 210 ℃ to 1 000 μL·L^{-1} NH_3.

Key words: $CoWO_4$; hydrothermal method; nanorods; nanocubes; gas-sensing property

收稿日期:2014-01-02。收修改稿日期:2014-04-07。
广西青年科学基金(桂科青 0991086)、国家自然科学基金(NSFC61271156)资助项目。
*通讯联系人。E-mail:auqfai@glmc.edu.cn

0 Introduction

The $CoWO_4$ crystal has a wolframite-like monoclinic structure and belongs to the *P*2/*a* (13) space group. Currently, many literatures have reported $CoWO_4/WO_3$ composite oxides as precursors to develop high quality WC-Co hard alloy, however, reports involving the preparation and properties of the pure $CoWO_4$ material are rare.

Up to now, several methods have been used to prepare $CoWO_4$ such as solid phase method including conventional solid-state reaction method at high temperature[1], Low-temperature molten salt method[2], hydrothermal method[3-6], solvothermal method[7], co-precipitation method[8-11], spray pyrolysis method[12], polymeric precursor method[13], etc. Generally, the as-prepared $CoWO_4$ powders are almost nanoparticles[5,9-13]. Yet, $CoWO_4$ nanorods and hollow flowerlike nanostructures can be successfully prepared by hydrothermal method[3-4] and solvothermal method[7]. Zhen et al.[3] synthesized $CoWO_4$ nanorods with average diameter of 20 nm and lengths of 100 to 300 nm by a hydrothermal route using only $CoCl_2$ and Na_2WO_4 as reaction reagents and distilled water as solvents. Song et al.[4] also prepared $CoWO_4$ nanorods through the Sodium dodecyl sulfate (SDS) assisted hydrothermal process at 453 K. You et al.[7] successfully prepared hollow flowerlike $CoWO_4$ by a simple reaction between $CoCl_2$ and freshly prepared H_2WO_4 in a single alcohol or Methanol or *n*-Octanol system without any surfactants. Obviously, the morphology of $CoWO_4$ can be regulated by adjusting the reaction conditions of hydrothermal method or solvothermal method. However, to the best of our knowledge, systematic investigation about the influence of different hydrothermal reaction conditions including the pH value of the reaction mixture, reaction time and reaction temperature on the phase and morphology of the as-prepared $CoWO_4$ has never been reported.

So far, only a few articles have reported microwave dielectric properties[14], luminescence properties[2,4,6,10,12] and catalytic properties[8-9,11] of $CoWO_4$. In addition, Kärkkänen et al.[15] fabricated a series of $CoWO_4$ (thickness ~100 nm) by pulsed laser deposition (PLD) and investigated the sensitivity of the films to CO. Diao et al.[13] demonstrated that the sensor based on $CoWO_4$ shows the largest response to NH_3 at elevated temperature with the 90% response and recovery time to 100 $\mu L \cdot L^{-1}$ NH_3 being only 3 s and 1 s, respectively. It seems that $CoWO_4$ reveals potential applications in sensor, therefore, more effort is needed to explore the gas-sensing properties of $CoWO_4$ materials.

Herein, in this paper, we describe the synthesis of $CoWO_4$ irregular nanoparticles, nanocubes and nanorods via a hydrothermal route using $Co(NO_3)_2 \cdot 6H_2O$, $Na_2WO_4 \cdot 2H_2O$ as the main raw materials and distilled water as the solvent without any surfactants. To the authors knowledge, $CoWO_4$ nanocubes have been fabricated for the first time. More importantly, we find that the morphology of products can be easily controlled by adjusting the pH value of the reaction mixture, reaction time and reaction temperature. Moreover, we investigate the gas-sensing property of the as-obtained $CoWO_4$ irregular nanoparticles, nanocubes and nanorods.

1 Experimental

1.1 Synthesis of $CoWO_4$ powders

The raw materials were of analytical grade reagents and used without further purification. In a typical process, 15.0 mL of 0.2 $mol \cdot L^{-1}$ Na_2WO_4 aqueous solution was added drop-wise into 15.0 mL of 0.2 $mol \cdot L^{-1}$ $Co(NO_3)_2$ aqueous solution with magnetic stirring. Then, dilute HNO_3 or NaOH solution (1 $mol \cdot L^{-1}$) or deionized water was added into the precursor suspension to adjust the pH to designed value. After stirring for 20 min, the final mixture was directly transferred into a 50 mL Teflon-lined stainless autoclave, filled up to 80% of its capacity. The autoclave was maintained at designed temperature for different times in an oven and then cooled naturally to room temperature. The precipitate was collected, washed with deionized water and absolute ethanol several times. After drying in air at 75 ℃ for 4 h, the

final powders were obtained.

To explore the influence of the hydrothermal reaction conditions including pH value, reaction time and reaction temperature to the products, a series of experiments were carried out, in which one parameter was variable and other reaction parameters were kept constant.

1.2 Characterization

The phase compositions of the as-synthesized products were examined by a Rigaku D/max 2500V X-ray diffractometer at the voltage of 40 kV and current of 200 mA with graphite monochromatized Cu $K\alpha$ radiation (λ=0.154 18 nm). Samples were tested at a scan rate of $10°\cdot min^{-1}$ with the scanning 2θ angles from 10° to 80°. The nanostructures of the powders were observed by transmission electronic microscopy (TEM) using a FEI-Tecnai 12 transmission electron microscope with an accelerating voltage of 100 kV. The specific surface areas were determined by N_2 adsorption-desorption at −196 ℃ using a Micromeritics ASAP 2420 analyzer.

1.3 Fabrication and measurement of gas-sensing property of sensors

The fabrication procedure of side-heated gas sensors was as follows: Firstly, the $CoWO_4$ products were ground with terpineol to form a homogeneous paste. Afterwards, the paste was coated on an Al_2O_3 tube with a diameter of 2 mm and length of 8 mm, which was previously positioned with one Au electrodes and two Pt wires on each end. Then it was heated in air at 100 ℃ for 10 h to remove the terpineol. After that, a Ni-Cr alloy wire was inserted into the Al_2O_3 tube as a heater, which provided the working temperature (100~500 ℃) of the gas sensor by tuning the heating voltage. Finally, the Al_2O_3 tube was welded onto a pedestal with six probes.

Electrical resistance of the sensor was measured in air and in sample gases. The sample gas was prepared via a stationary state gas distribution process: a glass chamber was vacuumized to about 50~80 kPa, a given amount of the gas (or liquid) to be detected was injected to the chamber, and then air was put into the chamber to let the pressure in the chamber to be 101.3 kPa. The gas concentration in the chamber could be calculated according to the gas volume injected and the chamber volume. The response (S) was defined as the ratio of the electrical resistance in air (R_a) to that in a sample gas (R_g), *i.e.* $S=R_a/R_g$.

2 Results and discussion

2.1 Effect of pH value on the phase compositions and morphologies of the products

Fig.1 shows the XRD patterns of the $CoWO_4$ powders prepared at 160 ℃ for 48 h with different pH values. It could be seen from Fig.1 that the pH value of the precursor mixture has a crucial influence on the formation of the tungstate phase in the hydrothermal process. Obviously, wolframite $CoWO_4$ is obtained when the pH value is in the range of 6~8. When the pH value is between 7 and 8, all the main diffraction peaks can be perfectly indexed to the monoclinic cell of $CoWO_4$ (PDF No. 15-0867), indicating that pure phases of $CoWO_4$ are obtained. However, when the pH value is 6, several characteristic peaks (noting with *) from impurities are detected, indicating that the products are not pure. Upon raising the pH value to the range of 9~12, the products are not $CoWO_4$. When the pH value is 12, there are peaks of $Co(OH)_2$ (PDF: 30-0443) in the XRD patterns, while when the pH value is adjusted from 9 to 11, the products can not be determined by checking the standard PDF cards now because no corresponding standard cards can be indexed.

Fig.2 shows the TEM images of the as-prepared

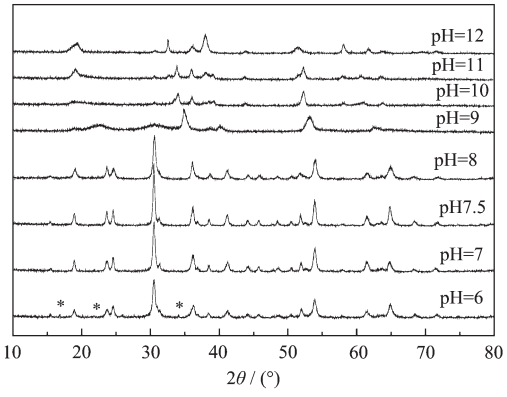

Fig.1　XRD patterns of the as-prepared powders at 160 ℃ for 48 h with different pH values

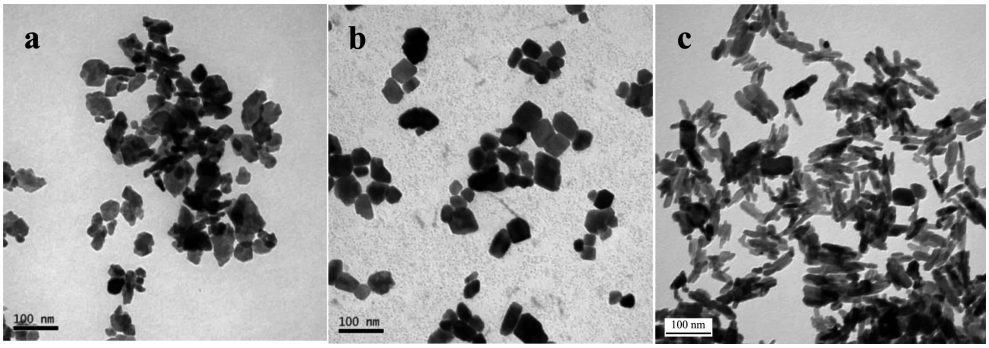

a: pH=7; b: pH=7.5; c: pH=8

Fig.2 TEM images of the as-prepared $CoWO_4$ powders at 160 ℃ for 48 h with different pH values

powders at different pH values (160 ℃, 48 h). It is obvious that the pH value exerts a significant influence on the morphology of $CoWO_4$. When the pH value is 7, as shown in Fig.2a, the product mainly consists of irregular nanoparticles (the particle size being about 10 ~100 nm), there are also a few nanorods in the sample. As illustrated in Fig.2b, the shape of particles is similar to nanocube when the pH value is increased to 7.5, the side length being about 20 ~80 nm. Further increasing the pH value of the precursor mixture to 8, nanorods with diameters of about 20 nm and lengths ranging between 40 and 140 nm are obtained, as depicted in Fig.2c, a few irregular and cubic shape nanoparticles appear in the sample at the same time.

2.2 Effect of hydrothermal temperature on the phase compositions and morphologies of the products

The XRD patterns of the as-synthesized powders prepared at different temperatures (pH=8, 24 h) are shown in Fig.3. The pure $CoWO_4$ can be prepared when the hydrothermal reaction temperature is from 130 ℃ to 180 ℃. Additionally, with the reaction temperature increasing, the diffraction peaks become stronger and sharper, indicating that the obtained products are well crystallized. However, whether there are any amorphous $CoWO_4$ in the products obtained at low reaction temperature can not be confirmed.

The TEM images of the as-prepared $CoWO_4$ powders collected at different temperatures (pH=8, 24 h) are displayed in Fig.4. The samples prepared at

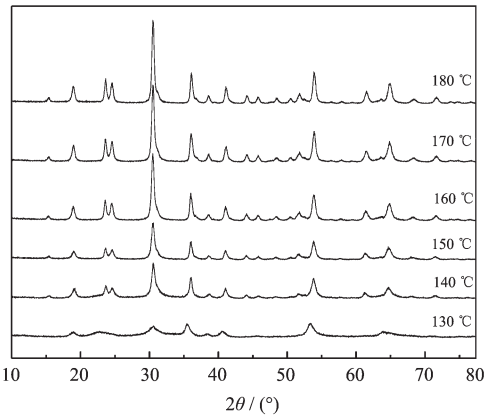

Fig.3 XRD patterns of the as-prepared powders at different temperatures with pH=8 for 24 h

140 ℃ are mainly irregular nanoparticles (Fig.4a). When the reaction temperature is 160 ℃, as shown in Fig.4b, the morphologies of synthesized $CoWO_4$ are nanorods (diameters of 10~20 nm and lengths of 20~120 nm) mixed with a few irregular and cubic shape nanoparticles. As the reaction temperature reaches 180 ℃, the TEM image (Fig.4c) shows that the products are almost nanorods with diameters of about 20 ~30 nm and lengths of 20 ~180 nm with rare irregular and cubic shape nanoparticles. In conclusion, the morphologies of products are affected by the hydrothermal temperature. As the hydrothermal temperature elevating from 140 ℃ to 180 ℃, irregular nanoparticles and nanorods emerge, and the nanorods become bigger and longer. Increasing the reaction temperature also results in a better crystallization of the products, which is similar to that speculated according to the XRD patterns.

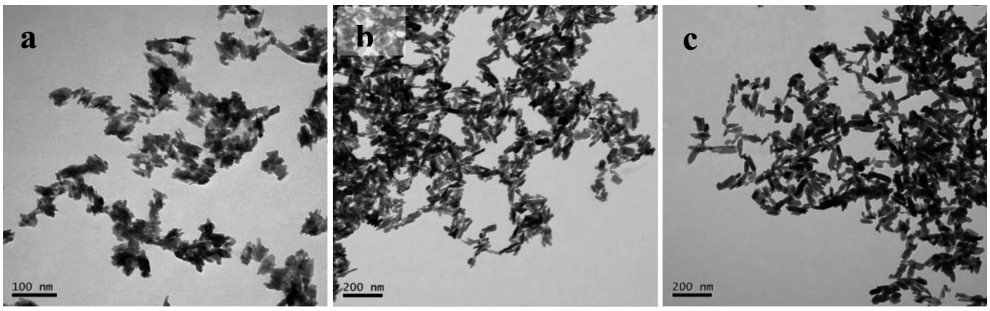

a: 140 ℃; b: 160 ℃; c: 180 ℃

Fig.4　TEM images of the as-prepared $CoWO_4$ powders at different temperatures with pH=8 for 24 h

2.3 Effect of reaction time on the phase compositions and morphologies of the products

Fig.5 shows the XRD patterns of the products obtained at different reaction periods, while the pH value of the reaction mixture and the hydrothermal temperature remain the same (pH=8, 160 ℃). Fig.5 reveals that pure wolframite $CoWO_4$ can be formed when the hydrothermal time is only 2 h (pH=8, 160 ℃). Apparently, keeping other reaction parameters constant and extending the reaction time (2 h~4 d), the diffraction peaks coincide well with the standard data of $CoWO_4$ (PDF card 15-0867), and the peaks become stronger and sharper suggesting an increase of crystallinity.

The TEM images of the samples prepared under the same hydrothermal temperature (160 ℃), same pH value (8) and different reaction times are shown in Fig.6. Clearly, the morphology of the products changes when the reaction time is extended. After hydrothermal treatment for 6 h (Fig.6a), the as-prepared $CoWO_4$ are mainly irregular nanoparticles with a small amount of nanorods (diameters of 5~10 nm and lengths of 20~50 nm). By increasing the reaction time to 12 h, abundant nanorods appear in the TEM image (Fig.6b) with diameters of about 10~15 nm and lengths of 30~80 nm. When the reaction time is extended to 24 h, abundant separate nanorods are formed, meanwhile, a small quantity of nanocubes and irregular nanoparticles are observed (Fig.6c). Further increasing the reaction time to 96 h, the nanocubes and irregular nanoparticles disappear, while nanorods with diameters of about 20~30 nm and lengths of 30~200 nm become the exclusive product, as shown in Fig.6d. Thereby, presumably, with the reaction time increasing from 6 h to 96 h, irregular particles generate firstly, and then the particles develop along some crystal axis/crystal face and gradually form nanorods.

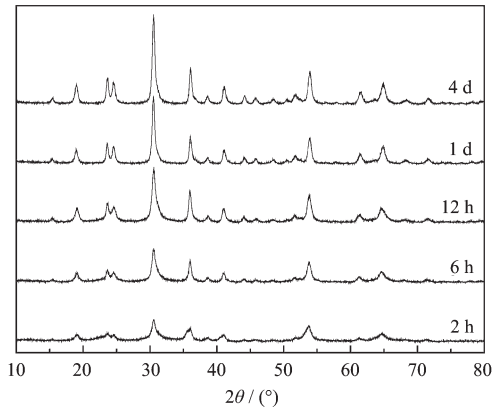

Fig.5　XRD patterns of the as-prepared powders at 160 ℃ with pH=8 for different reaction times

The above data suggest that the phase compositions of the products strongly depend on the hydrothermal reaction conditions, especially the initial pH value of the reaction mixture. Yu et al.[16] reported MWO_4 (M=Zn, Mn, Fe) nanorods/nanowires prepared by a similar hydrothermal method and pointed out that the involved reactions were "pH-dependent competing reactions". Similarly, the variation of phase compositions of our products with initial pH value can be explained by this theory.

The crystal growth is controlled by the extrinsic and intrinsic factors. Evidently, the morphologies of

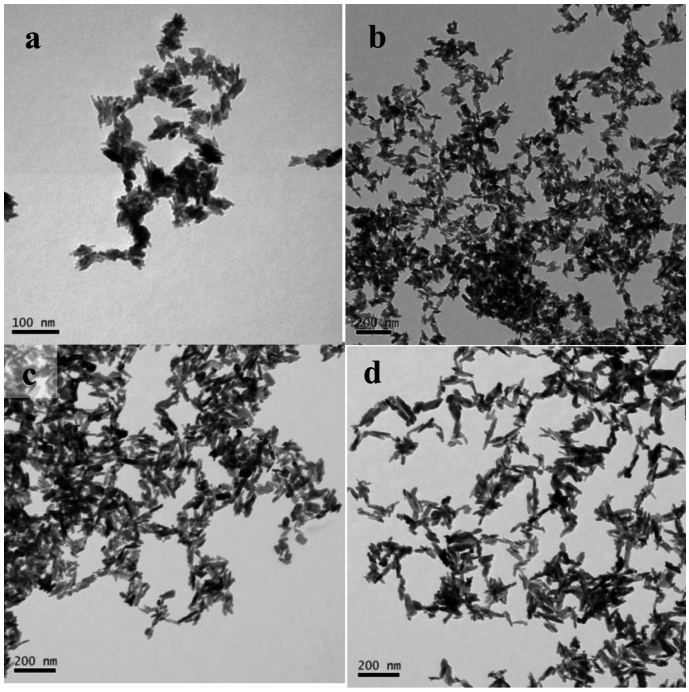

a: 6 h; b: 12 h; c: 24 h; d: 96 h

Fig.6 TEM images of the as-prepared $CoWO_4$ powders at 160 ℃ with pH=8 for different reaction times

$CoWO_4$ depend on the initial pH value as well as the reaction time and the reaction temperature. These extrinsic factors, especially the pH values may affect the growth rate of different crystal faces of $CoWO_4$ and cause some faces preferred orientation growth, leading to the formation of $CoWO_4$ with different morphologies. The TEM images of as-prepared $CoWO_4$ powders at 160 ℃ with pH=8 for different reaction times (6~96 h) demonstrate that the formation process of $CoWO_4$ nanorods is a typical Oswald ripening process, which is similar to the formation process of $ZnWO_4$ nanorods [17]. At the very beginning, $CoWO_4$ tiny crystalline nuclei forms in a highly supersaturates solution and this is followed by crystal growth. The larger particles grow at the cost of the small ones due to a higher solubility of the smaller particles. At the early stage, the coexistence of the short rods and irregular nanoparticles is found in the products. With reaction time extending, the irregular nanoparticles vanish and the longer nanorods form, suggesting that the longer nanorods grow at the expense of smaller particles. As for the formation mechanism of the $CoWO_4$ nanocubes, however, the direct proof has not obtained, and the detailed formation process is not very clear and needs further investigation.

2.4 Gas sensing performance

Gas sensors were fabricated using the $CoWO_4$ samples obtained via hydrothermal route at 160 ℃ for 48 h with pH value of 7, 7.5 or 8. As shown in Fig.2, the three samples represent irregular nanoparticles, nanocubes and nanorods, respectively. Their corresponding gas sensing performance was systematically investigated to different vapors including 1 000 $\mu L \cdot L^{-1}$ HCHO, C_2H_5OH, NH_3, C_6H_6 and CH_3COCH_3.

The responses to the detected gases of the three sensors at different operating temperatures are shown in Fig.7. Obviously, when the operating temperature is 120~300 ℃, the resistance of the sensors increases in a reducing atmosphere, indicating the senors are n-type semiconductors. The sensor based on irregular nanoparticles shows the best sensing property in contrast to the other two. However, the responses of the three sensors are low, the maximum being only 3.3, declaring their poor sensitivity to the tested gases. Diao et al.[13] reported that $CoWO_4$ materials prepared

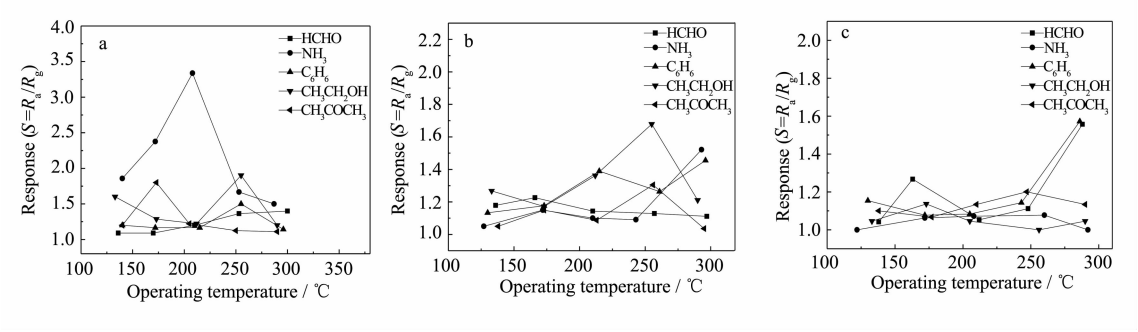

a. Irregular nanoparticles (pH=7,160 ℃, 2 d); b. Nanocubes (pH=7.5, 160 ℃, 2 d); c. Nanorods (pH=8, 160 ℃, 2 d)

Fig.7　Responses of the $CoWO_4$ sensors to 1 mL·L^{-1} various gases

by polymeric precursor method showed fast response and recovery characteristics and large sensitivity to NH_3 at elevated temperature (700 ℃). By contrast, our sensors exhibit response (the maximum being 3.3, Fig. 7a) to NH_3 at lower operating temperature, whereas the sensitivity and selectivity of our sensors is unsatisfactory, which needs to be further improved.

In addition, nitrogen adsorption-desorption analysis was exploited to measure the specific surface area of the above three samples. The BET specific surface area of the irregular nanoparticles, the nanocubes and the nanorods samples are calculated to be 41, 36 and 32 $m^2 \cdot g^{-1}$, respectively. Generally, larger specific surface areas may provide abundant space and more active sites for gas adsorption and surface contact reactions[18-19] between adsorbed oxygen ions and detected gases, which may cause a higher response. Thus, the highest response to NH_3 of the sensor based on irregular nanopaticles sample among the three kind sensors (Fig.7) may relevant to its largest specific surface area.

3　Conclusions

In summary, we fabricated $CoWO_4$ irregular nanoparticles, nanocubes and nanorods via a facile hydrothermal route in a simple reaction system of $Co(NO_3)_2$ and Na_2WO_4 without any surfactants. The results demonstrate that pH value, reaction temperature and hydrothermal time significantly affect the phase and morphology of the as-prepared $CoWO_4$ nano-crystallites. Pure $CoWO_4$ could be synthesized with the pH value of 7~8, the reaction temperature from 140 ℃ to 180 ℃, and the hydrothermal time longer than 2 h. Generally, $CoWO_4$ irregular nanoparticles, nanocubes and nanorods could be obtained with the pH value of 7, 7.5 and 8, respectively, for the reaction mixture. However, when the operating temperature is set as 120~300 ℃, the sensors based on $CoWO_4$ irregular nanoparticles, nanocubes and nanorods exhibit low responses to the tested gases. Further work is needed to improve the sensitivity and selectivity of the $CoWO_4$ materials.

References:

[1] Guo Q T, Wang J W, Kleppa O J. *Thermochim. Acta*, **2001**, **380**(1):1-4

[2] Song Z W, Ma J F, Sun H Y, et al. *Mater. Sci. Eng. B*, **2009**,**163**(1):62-65

[3] Zhen L, Wang W S, Xu C Y, et al. *Mater. Lett*., **2008**,**62**(10/11):1740-1742

[4] Song X C, Yang E, Ma R, et al. *J. Nanopart. Res*., **2008**,**10**(4):709-713

[5] Rajagopal S, Nataraj D, Khyzhun O Yu, et al. *J. Alloys Compd*., **2010**,**493**(1/2):340-345

[6] Zhang C L, Guo D L, Hu C G, et al. *Phys. Rev. B*, **2013**,**87**:035416

[7] You T, Cao G X, Song X Y, et al. *Mater. Lett.*, **2008**,**62**(8/9):1169-1172

[8] Montini T, Gombac V, Hameed A, et al. *Chem. Phys. Lett.*, **2010**,**498**(1/2/3):113-119

[9] Naik S J, Salker A V. *Catal. Commun.*, **2009**,**10**(6):884-888

[10]Naik S J, Salker A V. *Solid State Sci*., **2010**,**12**(12):2065-2072

[11]Garcia-Perez U M, Martinez-de la Cruz A, Peral J.

Electrochim. Acta, **2012**,**81**:227- 232

[12]Thongtem S, Wannapop S, Thongtem T. *Ceram. Int*., **2009**, **35**(5):2087-2091

[13]Diao Q, Fasheng Yang F S, Yin C G, et al. *Solid State Ionics*, **2012**,**225**:328-331

[14]Pullar R C, Farrah S, Alford N McN. *J. Eur. Ceram. Soc*., **2007**,**27**(2/3):1059-1063

[15]Kärkkänen I, Kodu M, Avarmaa T, et al. *Procedia Eng*., **2010**,**5**:160-163

[16]Yu S H, Liu B, Mo M S, et al. *Adv. Funct.Mater*., **2003**,**13** (8):639-647

[17]Liu B, Yu S H, Li L J, et al. *J. Phys. Chem. B*, **2004**,**108**(9): 2788-2792

[18]LI Lei(李蕾), ZENG Su-Yuan(曾涞源), MI Yu-Wei(米玉伟), et al. *Chinese J. Inorg. Chem.*(无机化学学报), **2012**,**28**(8): 1643-1650

[19]Liu Q, Yang Y, Sun B, et al. *Sens. Actuators*, *B*, **2014**,**194**: 27-32